Dynamics of seismogenic volcanic extrusion, Mount St. Helens, 2004-2005

R.M. Iverson[1], D. Dzurisin[1], C.A. Gardner[1], T.M. Gerlach[1], R.G. LaHusen[1], M. Lisowski[1], J.J. Major[1], S.D. Malone[2], J.A. Messerich[3], S.C. Moran[1], J.S. Pallister[1], A.I. Qamar[2,4], S.P. Schilling[1], J.W. Vallance[1]

SUMMARY

The 2004-2005 eruption of Mount St. Helens exhibited sustained, near-equilibrium behaviour characterized by nearly steady extrusion of a solid dacite plug and nearly periodic shallow earthquakes. Diverse data motivate the hypothesis that these earthquakes resulted from stick-slip motion along the margins of the plug as it was forced incrementally upward by ascending, solidifying, gas-poor magma. We formalize this hypothesis with a dynamical model that reveals a strong analogy between behaviour of the magma-plug system and that of a variably damped oscillator. Small oscillations in extrusion velocity grow unstably because plug friction exhibits rate weakening, but friction reverses direction when magma pressure relaxes sufficiently and the plug velocity declines to zero. This reversal transforms unstable oscillations into repetitive stick-slip cycles, irrespective of other frictional effects. Dynamical attraction to this self-regulating behaviour is strong, and inferred magnitudes of recurrent slip events help constrain the balance of forces governing the earthquakes and eruption.

---

[1]U.S. Geological Survey, Cascades Volcano Observatory, 1300 SE Cardinal Ct. #100, Vancouver, Washington 98683, USA; [2] Earth and Space Sciences, University of Washington, Seattle, Washington 98195, USA; [3] U.S. Geological Survey, Denver Federal Center, Box 25046, Lakewood, Colorado 80225, USA; [4]deceased

Silicic volcanoes are famous for explosions and other disequilibrium behaviour, but the dome-building eruption of Mount St. Helens (MSH) that began in October 2004 and continues today has exhibited prolonged, near-equilibrium behaviour that affords unique opportunities for understanding volcano dynamics. A remarkable feature of the eruption has been persistence of nearly steady, solid-state extrusion (1- 2 m^3/s) accompanied by nearly periodic earthquakes with shallow (< 1 km) focal depths. The repetitive nature of these earthquakes implies the existence of a nondestructive seismic source, and it provides an exceptional opportunity to link seismicity and extrusion dynamics[1,2]. Here, we summarize seismic, geodetic, photogrammetric, petrologic, geochemical, and thermal data collected during the 2004-2005 MSH eruption, and we hypothesize a mechanistic link between magma influx, nearly steady extrusion, and nearly periodic earthquakes. A new mathematical model formalizes our hypothesis and reveals a strong analogy between the behaviour of MSH and that of variably damped oscillators. We exploit this analogy to probe unobserved aspects of eruption dynamics.

Eruptive behavior and seismicity

Although MSH erupted explosively on 18 May1980, dome-building activity that began in 2004 is consistent with the volcano's recent geologic history[3]. Over the past ~ 4000 years MSH has extruded rock at a mean rate ~ 0.2 m^3/s while constructing a 26 km^3 edifice composed primarily of andesite and dacite lava flows and domes and their detritus (Supplementary Figure 1). From 1980-1986 a dacite dome grew episodically in the 1980 crater, and its volume ultimately reached 74×10^6 cubic metres[4]. From 1987-2004 MSH

did not erupt, although at least six phreatic explosions occurred from 1989-1991[5]. Recurrent seismicity at depths of 2-8 km in the late 1980s and 1990s may have been associated with magma recharge, but did not lead to eruptions[6].

The current eruption began on 1 October 2004, when a small explosion formed a ~20 m diameter vent through a ~150-m-thick glacier that had grown in the southern part of the MSH crater since 1986[7,8,9]. The explosion was preceded by 8 days of increasingly intense seismicity at depths < 1 km, but deeper seismicity did not occur then and has not occurred subsequently. By 11 October explosions had largely ceased, seismic energy release had decreased to a rate about one-tenth that of the preceding two weeks, and extrusion of a solid dacite plug had begun[7] (Figure 1 and Supplementary Movies 1 and 2). Extrusion has subsequently continued, and by 15 December 2005 the volume of the resulting new lava dome was ~ 73 $\times 10^6$ m^3. This volume, added to that of the 1980-1986 lava dome, implies that the average MSH extrusion rate for the period 1980-2005 is similar to the 0.2 m^3/s average for the past 4000 years.

A remarkable feature of the 2004-2005 eruption was persistence of small (< M_D 2) earthquakes that recurred so regularly that we dubbed them "drumbeats" (Figure 2). The period between successive drumbeats shifted slowly with time, but was nearly always 30-300 s (Figure 3). Seismograms showed that drumbeat waveforms typically had impulsive, high-frequency onsets and low-frequency codas, consistent with a source that involves abrupt slip but not fracture of intact rock. Accurate location of drumbeat hypocenters was hindered by the geologic and topographic complexity of the MSH crater and small number of crater seismometers (Supplementary Figure 1), but within resolution

limits (~ 100 m), all drumbeats originated at depths < 1 km directly around or beneath the growing dome. Irregularly interspersed with the drumbeats were smaller and larger earthquakes ($\leq M_D$ 3.4) with differing seismic signatures, but these earthquakes rarely had any effect on drumbeat occurrence.

Accompanying the drumbeats, extrusion of solid dacite created a dome consisting of a series of spines with freshly exposed surfaces coated with fault gouge (i.e., granulated rock bearing multiple generations of subparallel striations and slickensides). The most prominent spine emerged in winter 2005 and had a remarkably smooth, symmetrical whaleback form (Figure 1 and Supplementary Movies 1 and 2), but most spines were partly obscured as they pushed past glacial ice and previously extruded rock.

While spines repeatedly formed and decrepitated, extrusion rates remained roughly constant (Figure 3). The volumetric extrusion rate inferred from intermittent photogrammetic surveys was as high as ~ 6 m^3/s during the first several weeks of the eruption, but by December 2004 it had declined to a value of 1-2 m^3/s that was sustained for the ensuing year. (Measurement methods are described in Supplementary Material.) Similarly, the speed of plug emergence from the vent was nearly constant over timescales ranging from several minutes to several months and was typically 3-6 m/day (Figure 3). Safety concerns prevented close-up deployment of instruments capable of resolving mm-scale plug emergence inferred to occur over shorter timescales.

Character of extruded rock, gouge, and magma

Sampling of both the fault gouge coating the spines and the dacite beneath the gouge was accomplished mostly by dredging from a hovering helicopter. The gouge thickness was typically ~ 1 m and grain sizes were generally 0.001 - 10 mm. The gouge composition was similar to that of the newly erupted dacite, but included some constituents like those of pre-1980 MSH rocks. Airborne measurements of infrared radiation emitted by gouge emerging from the vent typically yielded temperatures ~ 200° C (Figure 1), and temperatures within fissures penetrating through the gouge were no higher than 730° C. Initial results of rheological experiments on the new dacite showed that even at a temperature of 1000º C, it deformed mostly by brittle failure, rather than viscous flow, accentuating the potential for strain localization, wear, and fault-gouge development[10, 11]. Room-temperature ring-shear tests on gouge specimens 7 cm thick under normal stresses of 86 to 191 kPa yielded steady-state (large-strain) friction coefficients μ ranging from 0.42 to 0.47, peak (small-strain) friction coefficients 1-9% larger than μ, and a roughly logarithmic decline of μ as displacement rates increased from about 10^{-6} to 10^{-4} m/s [12].

The mineralogy and major- and trace-element compositions of the newly extruded dacite are similar to those of the youngest rocks of the MSH dome emplaced in the 1980s[10]. Moreover, Fe-Ti oxide equilibration temperatures of samples collected in early November 2004 are like those of the 1986 MSH dacites (840-850º C). Owing to these similarities and low magmatic gas emissions, we infer that much of the 2004-2005 dacite originated from magma remaining in the reservoir tapped by the 1980s eruption.

Nonetheless, the long-term magma history may be complex, as extruded rocks contain phenocrysts that range widely in age and inferred source depth[10].

Petrologic data indicate that magma solidification occurred at depths < 1 km. The groundmass of the newly erupted dacite consists largely of a microlite mosaic of quartz or tridymite, sodic plagioclase and anorthoclase, with minor amounts (<15%) of high-silica rhyolite glass. The glass composition plots between the 0.1 and 50 MPa cotectics of the modified quartz-albite-orthoclase phase diagram for Mount St. Helens dacites[13], and the presence of tridymite further constrains the late stages of solidification to pressures of 10-20 MPa (equivalent to lithostatic pressures at depths ~ 500-1000 m)[10].

Volcanic gases intermittently measured by aircraft[14] include CO_2, SO_2, and H_2S, and these measurements generally indicate the presence of magma with an exsolved gas content lower than that at MSH in the early 1980s. Following the explosion of 1 October 2004, H_2S and CO_2 above ambient levels were detected, but gas emission rates remained very low (< 150 metric tons/day (td^{-1}) CO_2 and < 8 td^{-1} H_2S). After extrusion began on 11 October, mean emission rates increased to about 650 td^{-1} CO_2 and 100 td^{-1} SO_2 (Figure 3). The cumulative CO_2 released through July 2005 (about 190 kt) indicates that the 2004-2005 magma was gas-saturated at 8 km depth[15], and it constrains the gas volume fraction at that depth to < 2% (assuming the 2004-2005 and 1980-86 MSH dacites have similar water contents of ~5 wt% in the rhyolitic melt fractions[13,15,16]). Calculations using established methods[15] indicate that the gas volume fraction grew during magma ascent and reached about 50% at ~1 km depth, where solidification began, and averaged ~12% between 1-8 km. Allowing for inevitable gas separation during extrusion, these results

are consistent with observed vesicle volume fractions of 11-34% in samples of the 2004-2005 dacite[10].

Geodetic constraints on magma source

Measured displacements of the volcano flanks and adjacent areas imply that the volume of magma evacuated from depths < 10 km was considerably less than the volume of extruded rock. No evidence of systematic pre-eruption surface displacement was found by GPS surveys in 2000 and 2003 of a 40-station network centered on the volcano, nor by continuous operation of GPS station JRO1, located 8 km north of the volcano (Supplementary Figure 1). Seismicity that heralded the eruption in late September 2004 was accompanied by only cm-scale downward and inward surface displacements at JRO1 (Figure 3). The displacement pattern measured at all stations corresponds well with that predicted by an elastic half-space model[17] that assumes pressure decrease within a vertically oriented, prolate spheroidal cavity with a mean depth of 8 km and volume loss $\sim 2\times10^7$ m^3 during the period from 1 October 2004 to 25 November 2005. This apparent volume loss is less than one-third the volume of rock extruded during the same period, and most of the apparent volume loss occurred prior to the onset of nearly steady extrusion in December 2004 (Figure 3), implying that magma recharge from a deep (> 10 km) source accompanied the eruption.

Mechanical hypothesis

To gain mechanical insight, we focus principally on the extended periods when the extrusion rate and drumbeat earthquake frequency remained nearly constant. We infer that extrusion was driven by a steady influx of magma from a deep, replenishing reservoir and was resisted by nearly constant friction along the margins of the gouge-coated, solid plug. We hypothesize that drumbeat earthquakes represent seismic radiation associated with repetitive stick-slip motion along the plug margins, and that the stick-slip cycles themselves represent mechanical oscillations about equilibrium. Although prior studies have invoked stick-slip behaviour to explain cyclical phenomena during volcanic eruptions[11,18,19,20], these studies have not quantified the causes and character of stick-slip dynamics.

Quantification of our hypothesis requires identification of pertinent assumptions, parameters, and variables (Figure 4). We assume that magma flows into the base of a feeder conduit (at 8 km depth, inferred from 1980-2000 seismicity) at a rate $Q = 2$ m^3/s. An effectively rigid plug of solidified magma occupies the upper part of the conduit (to about 0.5 km depth, as inferred from petrologic and seismic data), but the position of the base of the plug may change owing to plug motion and basal accretion at mass rate ρB, where ρ is the magma bulk density and B is the volumetric rate of magma solidification. We assume that the plug bulk density ρ_r is constant (2000 kg/m^3, inferred from dome-rock specimens), but that the plug mass m can evolve owing to differences between ρB and $\rho_r E$, where E is the volumetric rate of surface erosion. For simplicity we assume

that $\kappa = \rho B - \rho_r E$ is a constant; thus $m = m_0 + \kappa t$, where m_0 is the initial plug mass and t is time. We estimate the horizontal cross-sectional area of the base of the plug, A, to be 30,000 m^2 (obtained by dividing $Q = 2$ m^3/s by the linear extrusion velocity 7×10^{-5} m/s); this A value implies an effective vent diameter ~ 200 m, consistent with results of photogrammetric analyses of the evolving plug geometry (Supplementary Movie 1). We estimate the bulk compressibility of the underlying magma α_1 as ~10^{-7} Pa^{-1} (appropriate for a 12% mean bubble content[21]), and estimate the elastic compliance of the adjacent conduit walls α_2 as ~10^{-9} Pa^{-1} (appropriate for fractured rock). Although values of α_1 and α_2 are not tightly constrained, the bubbly magma is almost certainly much more compliant than the conduit walls or the plug itself, and magma compression therefore dominates elastic strain in the system. Extrusion is resisted by the plug weight mg and a friction force F. Dependent variables that evolve simultaneously during extrusion are the upward plug velocity u, magma pressure against the base of the plug p, mean magma density ρ, and volume of the magma-filled conduit V (Figure 4)

If drumbeat earthquakes result from incremental slip along the margins of the plug, then the mean slip distance per drumbeat is $\bar{u}T$, where $\bar{u}$ is the mean extrusion velocity and T is the period between drumbeats. On this basis we infer that individual slip events typically involve abrupt plug displacements ~ 5 mm at earthquake focal depths. Calculations allow us to test whether our mechanical hypothesis is consistent with periodic displacements of this size, although such small, brief displacements were not detectable by our instrumentation network.

Dynamical model

We formalize our hypothesis with a mathematical model based on (a) one-dimensional conservation laws describing the evolving mass and vertical momentum of the solid plug and underlying magma; (b) constitutive equations describing plug boundary friction and compressibilities of the magma and conduit walls; and (c) the assumption that Q is constant. For these conditions the governing equations reduce to

$$\frac{du}{dt} = -g + \frac{1}{m_0 + \kappa t}\,(pA - \kappa u - F) \tag{1}$$

$$\frac{dp}{dt} = \frac{-1/V}{\alpha_1 + \alpha_2}\,(Au + RB - Q) \tag{2}$$

$$\frac{dV}{dt} = \frac{\alpha_1}{\alpha_1 + \alpha_2}(Au + RB - Q) + Q - B \tag{3}$$

where $R = 1 - (\rho / \rho_r)$ is a nearly constant coefficient determined by an isothermal equation of state, $d\rho / \rho = \alpha_1\, dp$, and all other variables and parameters are defined above. (Detailed derivations and discussions of these equations are included as Supplementary Material.)

If the plug mass is constant ($\kappa = 0$) and the basal solidification rate equals the magma influx rate ($B = Q$), Eqs. 1-3 have a simple equilibrium solution describing steady plug extrusion with constant magma pressure, magma density, conduit volume, and plug friction ($u = (Q - RB)/A$, $p = (m_0 g + F)/A$, $\rho = \rho_0$, $V = V_0$). Key dynamics questions are whether such steady states are stable, whether persistently oscillating states that can produce drumbeat earthquakes are probable, and whether initial disequilibrium

states (which necessarily exist at the onset of volcanic eruptions) are attracted to steady or unsteady states.

Insight can be gained by approximating R as constant, differentiating Eq. 1, combining it with Eq. 2, and normalizing the result to obtain an equation describing damped, forced oscillations of the scaled extrusion velocity, $u' = u/[(Q - RB)/A]$:

$$(1 + Kt')\frac{d^2u'}{dt'^2} + 2D\frac{du'}{dt'} + \frac{u'}{V'} = \frac{1}{V'} - \frac{Kgt_0}{(Q - RB)/A} \tag{4}$$

Here $t' = t/t_0$, $V' = V/V_0$, and quantities that largely control the system's behavior are the characteristic time, t_0, dimensionless mass change, K, and dimensionless damping, D:

$$t_0 = \frac{[m_0(\alpha_1 + \alpha_2)V_0]^{1/2}}{A} \qquad K = \frac{\kappa t_0}{m_0} \qquad D = K + \frac{1}{2}\frac{t_0}{m_0}\frac{dF}{du} \tag{5}$$

Interpretation of Eqs. 4 and 5 is most straightforward if $K = 0$, $V = V_0$, and D is constant (implying that F is a continuous, linear function of u). In this case, exact solutions of Eq. 4 indicate that u' either equals 1 (the steady equilibrium state) or oscillates about equilibrium with period $T = 2\pi t_0$. Application of this formula yields reasonable predictions of the period between drumbeat earthquakes at MSH (T ~ 10-100 s results from use of best-estimate values $m_0 = 3 \times 10^{10}$ kg and $V_0 = 10^6 - 10^8$ m^3 along with the A and α values noted above), but a model as simple as Eq. 4 with constant D cannot explain the persistence of drumbeats. Solutions of Eq. 4 with constant D show that oscillations grow unstably if $D < 0$, decay to yield a stable, steady state if $D > 0$, and

persist indefinitely only in the physically improbable case with $D = 0$. These inferences are modified only slightly if the restrictions $K = 0$ and $V = V_0$ are relaxed.

Persistent oscillations are much more probable if D varies as a consequence of nonlinearly rate-dependent friction, which produces variable feedback. To illustrate effects of such feedback we use an especially simple nonlinear friction rule,

$$F = \mathrm{sgn}(u)\, F_0 \left(1 + c \sinh^{-1} \left| u / u_{ref} \right| \right) \tag{6}$$

in which sgn(u) denotes the sign of u, F_0 is the friction force at static limiting equilibrium (for details, see Supplementary Materials), c is a rate-dependence parameter ($|c| << 1$), and u_{ref} is a reference value of u. For $c < 0$, Eq. 6 describes a convex function with peak friction at $u = 0$ and approximately logarithmic decay of F for $\left| u / u_{ref} \right| > 1$ (Supplementary Figure 2). This function mimics key aspects of MSH fault-gouge friction measured in experiments[12], but it omits evolving state variables included in more elaborate friction models[22]. Equation 6 does, however, include a fundamental type of state dependence: F jumps between the values F_0 and $-F_0$ if decreasing u leads to $u = 0$, because gravity provides a potential for downward plug motion, which friction must oppose. When F jumps, the damping D effectively becomes infinite and prohibits downward settling of the plug, thereby truncating oscillations of u. This truncation transforms oscillatory instability to stick-slip instability, irrespective of other rate or state effects.

Numerical solutions of Eqs. 1-3 using a standard Runge-Kutta method[23] and incorporating Eq. 6 show how friction regulates periodic stick-slip cycles during

extrusion. In the examples we discuss here (which employ K= 0, B=Q=2 m^3/s, T=10 s, and $u_{ref} = 0.1(Q/A)$), values of D at the equilibrium slip rate $u_0 = Q/A$ completely determine the behavior of solutions. (These values of D are obtained by using Eq. 6 to find $[dF/du]_{u=u_0} = F_0\, c/u_{ref}[1+(u_0/u_{ref})^2]^{-1/2}$ and substituting this result in the definition of D given above.) For negative D values close to 0, oscillations in u appear first as growing sinusoids with period T, but transform to repetitive stick-slip cycles when u = 0 occurs (Supplementary Figure 3). As D becomes more negative, slip events become less frequent and more abrupt (Figure 5a).

Simultaneous evolution of u and p during stick-slip cycles reveals key features of extrusion dynamics (Figure 5b). When basal magma influx produces pressure exceeding the static equilibrium value ($p_0 = (m_0 g + F_0)/A$), it triggers slip at a rate that may slightly or greatly surpass the steady equilibrium rate Q/A, depending on the value of D. When a combination of plug inertia and diminishing magma pressure no longer suffices to overcome the effects of gravity and friction, slip terminates and stick begins. Magma pressure then rebuilds until it triggers another slip event.

Computations with $D = -2$ produce stick-slip cycles with amplitudes and periods similar to those inferred for MSH plug extrusion (Figure 5a). With $D = -2$, individual slip events entail about 5 mm of displacement in about 5 s, maximum slip rates ~ 2 mm/s, and about 10^8 J of work done against friction. Attendant fluctuations in magma pressure are < 0.02% of p_0 (Figure 5b), equivalent to only ~ 2500 Pa or < 0.2 m of static magma pressure head. This result is insensitive to variations in the parameters that constitute D,

provided that t_0 is unchanged (Supplementary Figures 4 and 5), and it implies that a remarkably delicate shift in the balance of forces distinguishes periods of slip from those with no slip. Multiplied by $A = 30,000$ m^3, the ~ 2500 Pa pressure change also serves as a proxy for the force drop responsible for generating seismicity ($\sim 8\times10^7$ N). Standard estimation methods indicate that this force drop, accompanying a displacement ~ 5 mm, would produce about 2×10^5 J of seismic energy radiation[24], consistent with the conclusion that only a small fraction of the work done during fault slip produces seismicity[25].

The dynamics of the magma-plug system are further illustrated by behavior in the *u*-*p* phase plane with disequilibrium initial conditions (Figure 6). If an eruption begins with excess magma pressure ($p > p_0$), an initial pulse of rapid motion occurs until pressure relaxes and static equilibrium is restored, irrespective of the sign or value of *D*. Pressure then rebuilds until it triggers a second stage of motion. For $D < 0$ this stage consists of endlessly repetitive stick-slip limit cycles (dashed line in Figure 6), whereas for $D > 0$ it converges to a fixed-point equilibrium representing a state with dynamically balanced forces (solid line in Figure 6). The size and speed of the initial movement pulse increases almost linearly with the initial excess pressure, and cases with rate-strengthening friction ($D > 0$) and rate-weakening friction ($D< 0$) exhibit similar pulses if the initial pressure disequilibrium is sufficiently large. Lack of large movement pulses at MSH implies that magma pressure exceeding p_0 by even a few percent has probably not been present during the 2004-2005 eruption.

Conclusion

All silicic volcanic eruptions that follow a period of repose begin with a plugged conduit. Commonly the conduit is rapidly cleared of solid rock, and a profoundly disequilibrated state exists as magma reaches the surface. In the 2004-2005 eruption of MSH, the conduit remained plugged by solid rock that was pushed upward by ascending, solidifying magma. The magma-plug system reached a sustained, near-equilibrium state characterized by nearly steady extrusion of gouge-coated dacite and nearly periodic drumbeat earthquakes. A dynamical model of the magma-plug system produces output consistent with the hypothesis that the drumbeats resulted from repetitive stick-slip motion along the margins of the extruding plug, and that the stick-slip cycles represent mechanical oscillations about equilibrium. Rate-weakening gouge friction and the potential for downward plug motion (due to gravity) suffice to produce stick-slip behaviour in this system.

Application of driving force by an unusually compliant body (i.e. bubbly magma) may play a crucial role in enabling stick-slip events to produce earthquakes at shallow focal depths (< 1 km) observed at MSH. If gouge displacement were driven by a stiffer body (i.e., solid rock), oscillations in extrusion rate would be smaller, more frequent, and more likely aseismic[12].

Evidence that the 2004-2005 eruption of MSH quickly settled into a persistent, near-equilibrium, oscillatory state implies that magma pressure never deviated much from the steady equilibrium pressure. Moreover, absence of deep earthquakes and

minimal far-field deformation imply minimal changes in the magmatic system at depth, and we infer that the volcano was probably poised in a near-eruptive equilibrium state long before the onset of the 2004-2005 eruption. In many respects, the 2004-2005 eruption can be viewed as a continuation of the dome-building eruption of 1980-1986, whereas the explosive eruption of 18 May 1980 differed greatly because it was triggered by a 2.5 km^3 landslide that rapidly depressurized volatile-rich magma.

The trigger of the 2004-2005 eruption remains unknown, but all evidence indicates that it was subtle. The eruption may have been triggered from below by an undetected increase in magma pressure or from above by exceptional late summer rain and glacier melt that increased groundwater pressures (perhaps aided by thermal effects) and thereby weakened the rock capping and bounding the volcanic conduit. This conjecture is less important, however, than is our conclusion that silicic volcanoes can exist in equilibrium states that differ very little during eruptive and noneruptive periods.

REFERENCES CITED

1. Lahr, J.C., Chouet, B.A., Stephens, C.D., Power, J.A., & Page, R.A. Earthquake classification, location, and error analysis in a volcanic environment: implications for the magmatic system of the 1989-1990 eruptions at Redoubt Volcano, Alaska. *J. Volcanology and Geothermal Res*. **62**, 137-151 (1994).

2. Neuberg, J. Characteristics and causes of shallow sesimicity in andesite volcanoes. *Phil. Trans. R. Soc. London A* **358**, 1533-1546 (2000).

3. Mullineaux, D.R., & Crandell, D.R. The eruptive history of Mount St. Helens, in *The 1980 Eruptions of Mount St. Helens, Washington* (eds. Lipman, P.L. and Mullineaux, D.R.) U.S. Geological Survey Professional Paper 1250, 3-15 (1981).

4. Swanson, D.A., & Holcomb, R.T. Regularities in growth of the Mount St. Helens dacite dome, in *Lava Flows and Domes* (ed. Fink, J.) 3-24 (Springer-Verlag, Berlin, 1990).

5. Mastin, L.G. Explosive tephra emissions at Mount St. Helens, 1989-1991; the violent escape of magmatic gas following storms? *Geol. Soc. Amer. Bull.* **106**, 175-185 (1994).

6. Moran, S.C. Seismicity at Mount St. Helens, 1987–1992: Evidence for repressurization of an active magmatic system. *J. Geophys. Res.* **99**, 4341-4354 (1994).

7. Dzurisin, D., Vallance, J.W., Gerlach, T.M., Moran, S.C. & Malone, S.D. Mount St. Helens reawakens. *EOS* **86**, 25&29 (2005).

8. Schilling, S.P., Carrara, P.E., Thompson, R.A., & Iwatsubo, E.Y. Posteruption glacier development within the crater of Mount St. Helens, Washington, USA. *Quaternary Research* **61**, 325-329 (2004).

9. Walder, J.S., LaHusen, R.G., Vallance, J.W. & Schilling, S.P. Crater glaciers on active volcanoes: hydrological anomalies. *EOS* **86**, 521&528 (2005).

10. Pallister, J.S., Reagan, M. & Cashman, K. A new eruptive cycle at Mount St. Helens? *EOS* **86**, 499 (2005).

11. Tuffen, H. & Dingwell, D. Fault textures in volcanic conduits: evidence for seismic trigger mechanisms during silicic eruptions. *Bull. Volcanology* **67**, 370-387 (2005).

12. Moore, P.L., Iverson, N.R. & Iverson, R.M. Frictional properties of the 2004-2005 Mount St. Helens gouge. accepted for publication in *A Volcano Rekindled: the first year of renewed eruption at Mount St. Helens, 2004-2005* (eds. D.A. Sherrod and W.E. Scott) U.S. Geological Survey Professional Paper, in preparation.

13. Blundy, J., & Cashman, K. Ascent-driven crystallization of dacite magmas at Mount St. Helens, 1980-1986. *Contrib. Mineral. Petrol.* **140**, 631-650 (2001).

14 McGee, K.A., Doukas, M.P., & Gerlach, T.M. Quiescent hydrogen sulfide and carbon dioxide degassing from Mount Baker, Washington. *Geophysical Res. Let.* **28**, 4479-4482 (2001).

15. Newman, S., & Lowenstern, J.A., VolatileCalc: a silicate melt-H_20-$C0_2$ solution model written in Visual Basic for Application (VBA) with Microsoft® Excel. *Computers and Geosciences* **28**, 597-604 (2002).

16. Rutherford, M.J. Experimental petrology applied to volcanic processes. *EOS* **74**, 49&55 (1993).

17. Yang, X., Davis, P.M., & Dieterich, J.H. Deformation from inflation of a dipping finite prolate spheroid in an elastic half space as a model for volcanic stressing. *J. Geophys. Res.* **93**, 4249-4257 (1988).

18. Denlinger, R.P. & Hoblitt, R.P. Cyclic eruptive behavior of silicic volcanoes. *Geology* **27**, 459-462 (1999).

19. Voight, B., and 24 others. Magma flow instability and cyclic activity at Soufriere Hills Volcano, Montserrat, British West Indies. *Science* **283**, 1138-1142 (1999).

20. Ozerov, A., Ispolatov, I., & Lees, J. Modeling Strombolian eruptions of Karymsky volcano, Kamchatka, Russia. *J. Volcanology Geotherm. Res.* **122**, 265-280 (2003).

21. Mastin, L.G. & Ghiorso, M.S. A numerical program for steady-state flow of magma-gas mixtures through vertical eruptive conduits. *U.S. Geol. Suvey Open-File Report 00-209*, 56 p (2000).

22. Marone, C. Laboratory-derived friction laws and their application to seismic faulting. *Ann. Rev. Earth Planet Sci.* **26**, 643-696 (1998).

23. Press, W.H., Flannery, B.P., Teukolsky, S.A. & Vettering, W.T. *Numerical Recipes the Art of Scientific Computing*. Cambridge, Cambridge University Press, 818 p (1986).

24. Scholz, C.H. *The Mechanics of Earthquakes and Faulting*, 2nd edition . Cambridge. Cambridge University Press, 471 p (2002).

25. McGarr, A. On relating apparent stress to the stress causing earthquake fault slip. *J. of Geophys. Res.* **104**, 3003-3011 (1999).

Acknowledgments: We are indebted to many colleagues, too numerous to name, who contributed to the response to the 2004-2005 eruptive activity at MSH.

FIGURE LEGENDS

Figure 1. Images of whaleback spine and surrounding MSH crater in February 2005.

(a) Oblique aerial view from the northwest. Arrow indicates vent from which whaleback emerged. Horizontal length of smooth whaleback is about 380 m. (b) Close-up view of gouge-covered surface of spine where it emerged from vent, viewed from the northeast. (c) Thermal infrared view from perspective similar to (b).

Figure 2. Sample 24-hour seismogram illustrating regular occurrence of "drumbeat" earthquakes. Graph shows seismicity recorded at station YEL, located 1.5 km north of the 2004-2005 vent (Supplementary Figure 1). Time begins at 21:00 UTC on 1 December 2005, and scrolls from left to right and then top to bottom. Earthquake magnitudes were roughly 0.5-1 during this interval.

Figure 3. Time-series data summarizing eruption behavior. (a) Cumulative volume of extruded rock. (b) Mean period (± 1 std. dev) between successive earthquakes recorded at station YEL (Supplementary Figure 1), computed for 24-hour sampling windows. (c) Linear extrusion rate ± 1 std. dev., inferred from repeat photography. Data gaps appear where clouds obscured view or equipment malfunctioned. (d) Emission rates of gaseous CO_2 and SO_2. (e) Cumulative southward displacement of continuous GPS station JRO1, located 9 km north of the vent (Supplementary Figure 1). Regional displacements due to plate tectonic motion (constrained by regional GPS) have been removed from data.

Figure 4. Model schematic.

Figure 5. Stick-slip extrusion behavior computed for various values of the parameter D depicted as (a) time series, and (b) limit cycles in the velocity-pressure phase plane. Arrows in (b) point in the direction of advancing time. Static equilibrium initial conditions (I.C.) for these calculations were specified by $u = 0$, $p = p_0 = 1.2936 \times 10^7$ Pa, $V = V_0 = 6.32 \times 10^5$ m^3, and $\rho = \rho_0 = 2000$ kg/m^3. Further discussion of calculations and parameter values is provided in Supplementary Materials.

Figure 6. Phase-plane diagram similar to that of Figure 5b computed for a static initial condition with disequilibrium pressure $p / p_0 = 1.00005$. Other initial conditions were the same as those used to generate Figure 5. Results are shown for both rate-strengthening friction ($D = 2$; solid line) and rate-weakening friction ($D = -2$; dashed line).

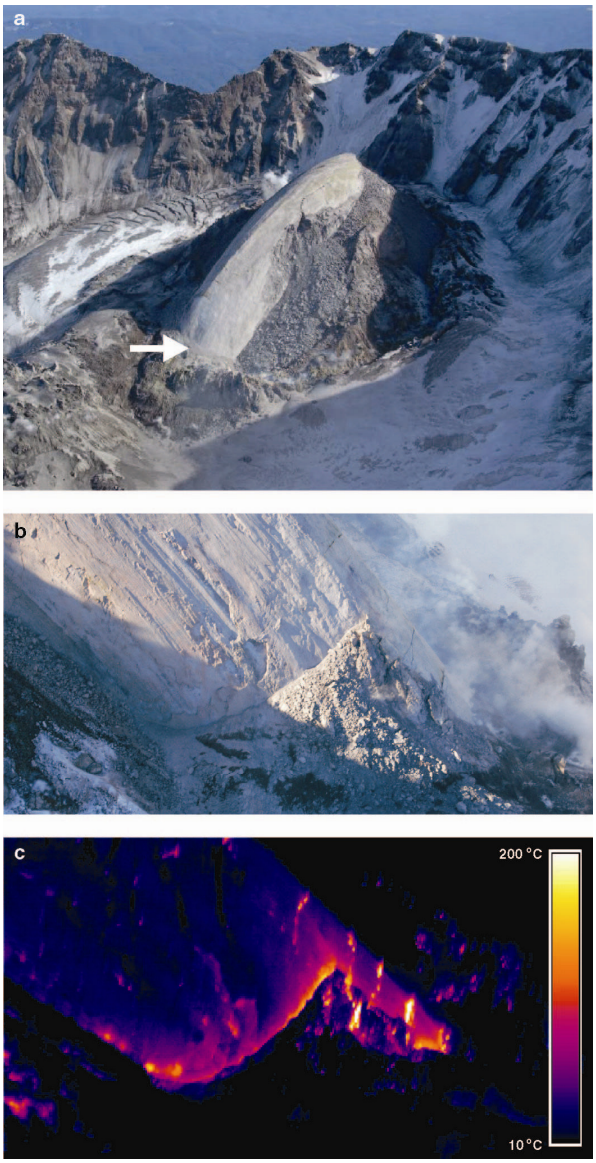

Figure 1.

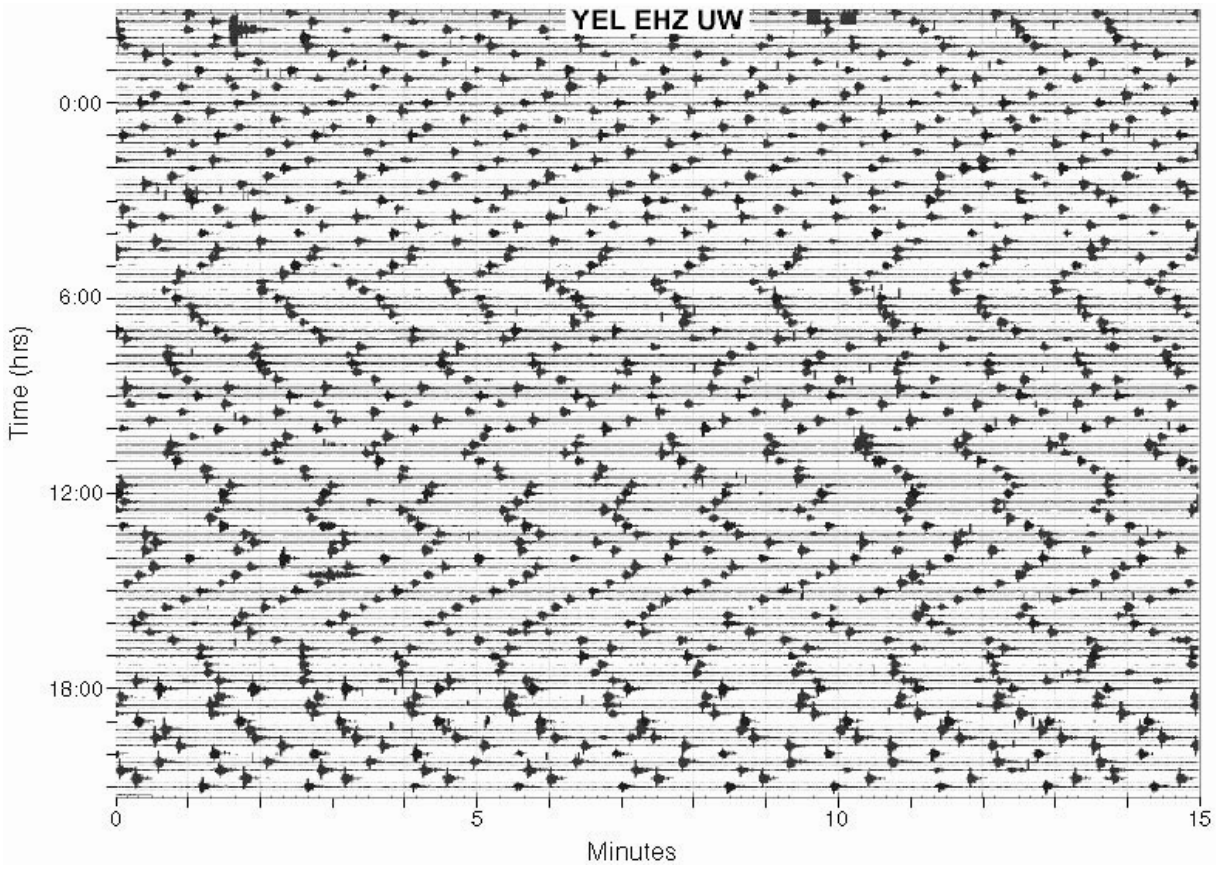

Figure 2.

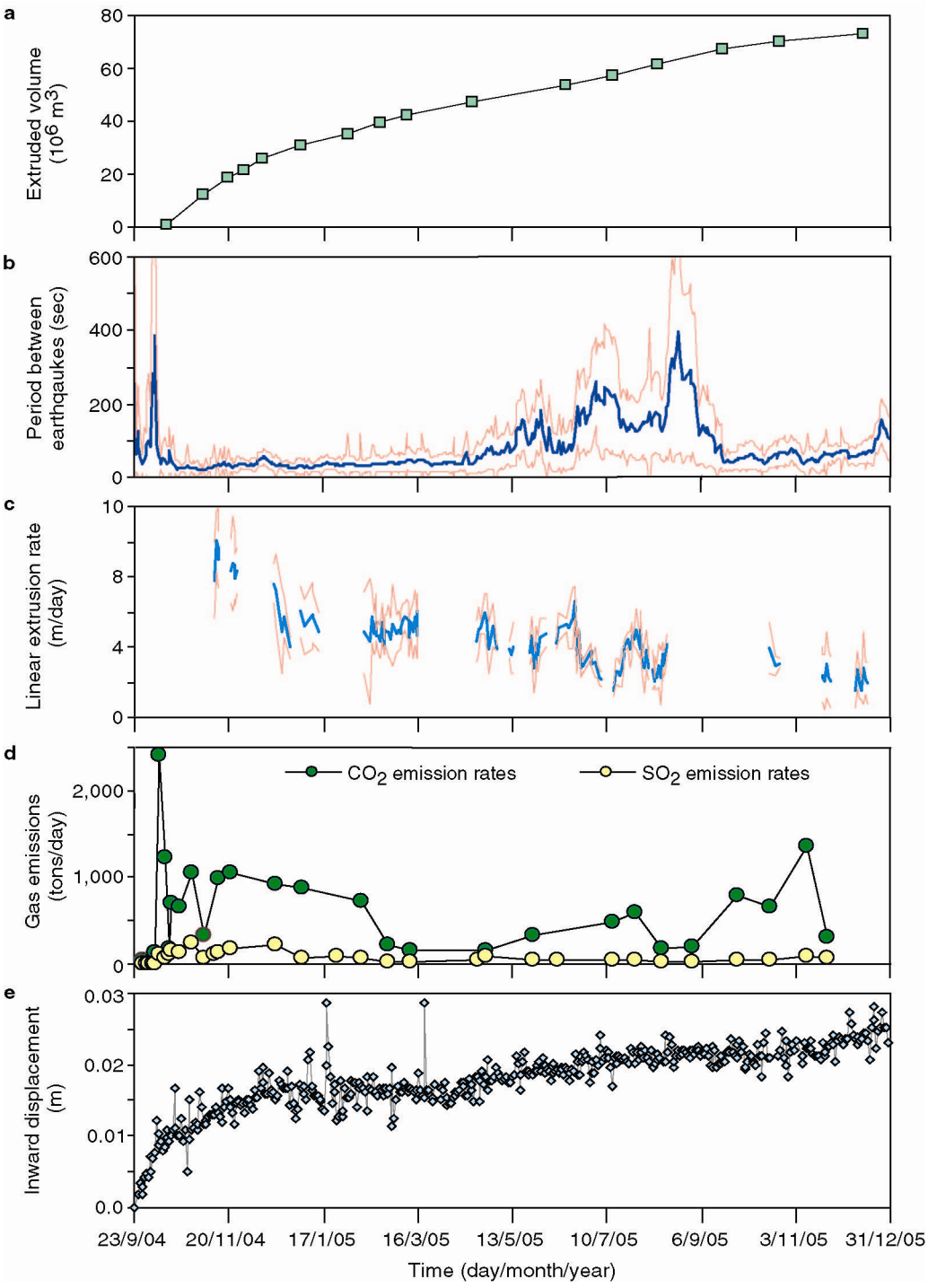
a
Extruded volume (10^6 m^3)
80
60
40
20
0
b
Period between earthquakes (sec)
600
400
200
0
c
Linear extrusion rate (m/day)
10
8
4
0
d
Gas emissions (tons/day)
CO_2 emission rates
SO_2 emission rates
2,000
1,000
0
e
Inward displacement (m)
0.03
0.02
0.01
0.0
23/9/04
20/11/04
17/1/05
16/3/05
13/5/05
10/7/05
6/9/05
3/11/05
31/12/05
Time (day/month/year)

Figure 3.

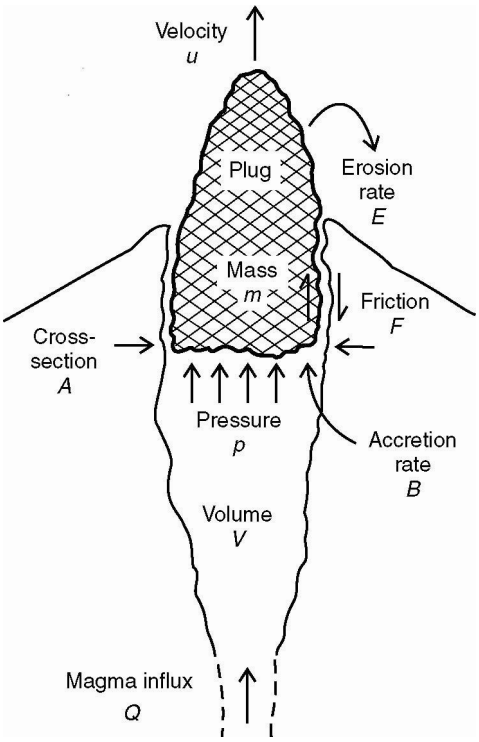
Velocity
u
Plug
Erosion
rate
E
Mass
m
Friction
F
Cross-
section
A
Pressure
p
Accretion
rate
B
Volume
V
Magma influx
Q

Figure 4.

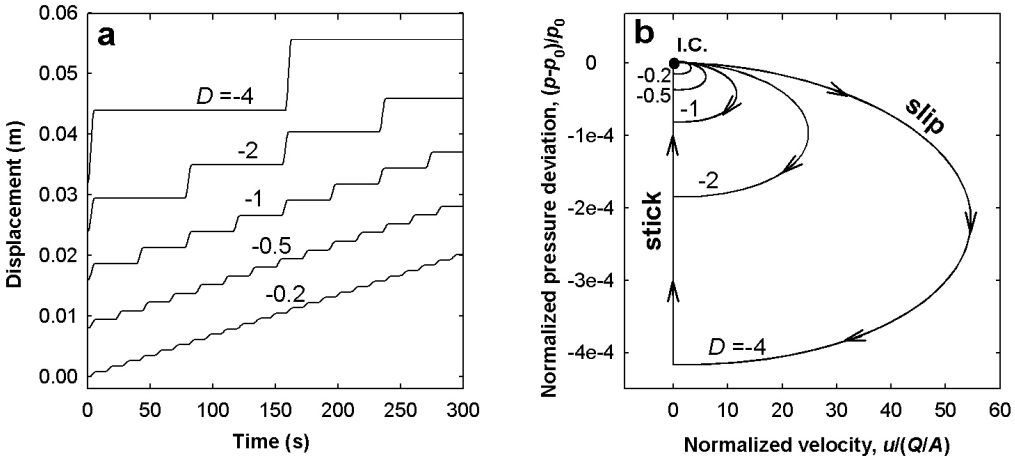
a
Displacement (m)
Time (s)
D =-4
-2
-1
-0.5
-0.2
b
Normalized pressure deviation, (p-p0)/p0
Normalized velocity, u/(Q/A)
I.C.
slip
stick
D =-4

Figure 5.

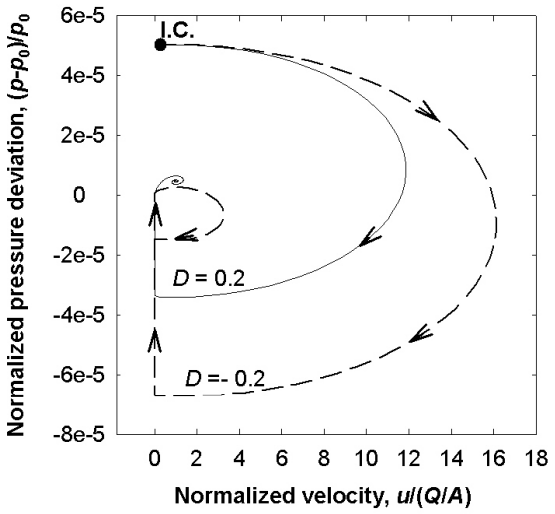
I.C.
D = 0.2
D =- 0.2
Normalized pressure deviation, (p-p0)/p0
Normalized velocity, u/(Q/A)
6e-5
4e-5
2e-5
0
-2e-5
-4e-5
-6e-5
-8e-5
0 2 4 6 8 10 12 14 16 18

Figure 6.